

Signature of Kondo effect in silicon quantum dots

M. Specht^{1,a}, M. Sanquer^{1,b}, S. Deleonibus², and G. Guégan²

¹ DRFMC-SPSMS, CEA-Grenoble, 38054 Grenoble Cedex 9, France

² CEA-LETI, CEA-Grenoble, 38054 Grenoble Cedex 9, France

Received 13 November 2001 and Received in final form 18 February 2002

Abstract. We report observation of the Kondo effect in the Coulomb blockade oscillations of an impurity quantum dot (IQD). This IQD is formed in the channel of a 100 nm gate length Silicon MOSFET. The quantitative analysis of the anomalous temperature and voltage dependence for the drain-source current over a series of Coulomb blockade oscillations is performed. It strongly supports the Kondo explanation for the conductance behavior at very low temperature in this standard microelectronics device.

PACS. 73.21.La Quantum dots – 73.23.Hk Coulomb blockade; Single-electron tunneling

Kondo effect has been reported in GaAs heterostructures (both in planar and vertical geometries) [1–6] and in carbon nanotubes [7]. It appears as a general property in small electronic systems with a well defined number of electrons strongly coupled to electrodes [8]. In the context of artificial quantum dots, Kondo effect is the manifestation of the spin polarized cotunneling effect. For large tunneling rate Γ through the dot, a Kondo resonance appears due to the coherent superposition of cotunneling events with spin-flip, which competes with the Coulomb blockade current through the dot. It has been demonstrated recently that the Kondo resonance can even suppress completely the Coulomb blockade [7,9]. If Γ is small, that means the dot is weakly connected to electrodes, cotunneling *i.e.* correlated transfer of two electrons through both tunnel barriers, is a small perturbation to Coulomb blockade (cotunneling goes like Γ^2 [10]). For large Γ , cotunneling becomes important and decreases the lifetime of the confined electronic state in the dot. If this state corresponds to an odd number of electrons of total spin $S = 1/2$, the increase of the tunneling rate is accompanied with a Kondo resonance. The Kondo temperature, which fixes the energy scale for the Kondo resonance in the valleys of conductances for an odd number of electrons in the dot (*i.e.* when the last single occupied state has an energy $\epsilon_0 = \mu - U/2$) is given by [8]:

$$k_B T_K = \frac{1}{2} (h\Gamma U)^{1/2} \exp\left(-\frac{\pi}{4} U/h\Gamma\right) \quad (1)$$

U is the charging energy ($U = e^2/C$ in the constant charging energy model). μ is the electrochemical potential fixed in the reservoirs. For an even number of electrons of total

spin $S = 0$, no Kondo resonance exists; the alternance of Kondo-Normal behaviors with the parity of the electrons number in the dot is a decisive experimental argument in favour of the model.

To get large Kondo temperature, the ratio $U/h\Gamma$ should be small enough. This ratio is minimized by U/Δ in quantum dots because $h\Gamma \leq \Delta$ is a necessary condition to define the number of electrons in the dot (this number is defined only if the conductance without Coulomb blockade, is less than e^2/h and the conductance is given by $g \simeq e^2/h \times (\frac{h\Gamma}{\Delta})$). $\Delta \simeq 1/\Omega\rho$ is the one particle mean level spacing in the dot (Ω is the volume of the dot and ρ the density of states). In metallic systems the density of states is very large, $\Delta \ll k_B T \ll U$, and the Kondo temperature is extremely small, not accessible experimentally. In GaAs 2 dimensional electron gas (2DEG), due to the small density of states $\rho_{2DEG} = m^*/\pi\hbar^2$, Δ is relatively large. Small dots are necessary to observe the Kondo effect because $U/\Delta \simeq U/h\Gamma$ decreases with the dot size.

The other nanosystem where Kondo effect is reported is the carbon nanotube [7], which are intermediate between GaAs and metallic structures as far as the density of states is concerned. Due to their quasi 1D structure and their small volume, the mean level spacing Δ is nevertheless relatively large.

Kondo effect has been previously reported in a small silicon impurity quantum dot (IQD), but the results are anomalous in many aspects, including the magnetic field dependence [11]. Spontaneous spin polarization has also been reported in the same system [12]. As compared to this system, our short and wide geometry makes our conducting channel less sensitive to effects due to multiple dots in series [11] (the dot is well connected to source and drain, see later on). We do not observe either a parallel conducting channel [12]. Both effects complicate the analysis in the Coulomb blockade regime.

^a Present address: Infineon Technologies AG, Otto-Hahn-Ring 6, 81730 Munich, Germany

^b e-mail: msanquer@cea.fr

Nevertheless Kondo effect is believed to be quite general and affects the low temperature electronic properties of any small system with a well defined number of electrons connected to electrodes [8]. We have shown previously that IQD appear in functional standard MOSFETs [13] and we report here that Kondo resonance exists in this silicon microelectronics context also.

For 2D silicon inversion channel, due to a larger effective mass and band degeneracies, ρ_{2DEG} is larger than in GaAs, that means smaller Δ , and smaller Kondo temperature. But on the other hand, IQD are smaller in size than artificial quantum dots, a favorable circumstance for Kondo resonance observation. In our systems the diameter is estimated to be 65 nm in 100 nm gate length MOSFET, and 40 nm in 50 nm gate length series [13].

Our MOSFETs are low mobility devices whose characteristics are described elsewhere [13]. Contrarily to the case of quasi-1D wires, the MOSFETs that we investigate are wide and short. In this study, the transverse size of the channel is 0.4 μm and the gate length is 100 nm only (the effective channel length is still smaller by typically 25 nm due to drain-source extension regions).

Below the threshold gate voltage, when the conductance is less than e^2/h , electrons experience a fluctuating disorder potential (by dopants in silicon and rugosity/defects in the gate oxide) whose amplitude of order 10 meV is comparable to their Fermi energy. A resonating IQD is probably a local statistical minimum in the acceptor Boron dopant concentration in the channel. If the tunnel conductances to the drain and source respectively are nearly equal (for instance if the IQD is centered between the drain and the source), it exhibits a resonant conductance which is exponentially larger than any other conducting channel in parallel, at least at low temperature. In particular, the transmission through such an IQD dominates completely over the direct tunneling and the tunneling through uncentered impurity quantum dots [14]. By the geometry itself, which is the dual of a quasi one dimensional silicon wire geometry, the IQD is well connected to the electrodes.

IQD in standard MOSFETs differ from artificial quantum dots in many aspects. Among them is the presence of a very thin gate dielectric SiO_2 layer of thickness $d_{\text{SiO}_2} = 3.8$ nm, much less than the estimated mean distance between electrons in the IQD, typically $r_{ee} = 10$ nm when the dot is completely filled with electrons [13]. The interaction energy U goes like the inverse of the gate capacitance in standard charging model, so is proportional to d_{SiO_2} . In the microscopic description of the gate screened dipolar Coulomb interaction, U goes like $d_{\text{SiO}_2}^2/r_{ee}^3$. In both cases U decreases with the gate oxide thickness, that characterizes the effect of the strong screening by the gate. Secondly, the electrodes are the heavily doped source and drain and their extension regions. These electrodes are good massive “reservoirs” for the electrons, contrarily to artificial quantum dots, where electrodes are also thin 2DEG. These characteristics are important in the context of the Kondo effect, which appears in the nearly open regime of the dot (so it is important to have low resistive

reservoirs) and for small value of U/Δ (U decreases with the gate oxide thickness, Δ being constant).

U , $h\Gamma$ and Δ , the important parameters for Kondo physics, are strongly dependent on the gate voltage in our IQD and can be estimated through the characteristics of the Coulomb blockade oscillations. The drain source current resonances we observe at low gate voltage correspond to electrons sitting at the bottom of the IQD potential. As in other lateral geometries, we do not know the absolute number of electrons in our IQD. In this low gate voltage regime, corresponding to the weakly connected case, the Coulomb blockade resonances are given by the Breit-Wigner Lorentzian form convoluted with the derivative of the Fermi distribution function. The Breit Wigner form for the conductance *versus* electron energy ϵ (counted from μ in the reservoirs) is [15]:

$$G(\epsilon) = \frac{e^2}{h} \frac{\Gamma_l \Gamma_r}{\Gamma_l + \Gamma_r} \frac{\Gamma}{(\epsilon/h)^2 + (\Gamma/2)^2} \quad (2)$$

$\Gamma = \Gamma_l + \Gamma_r$ is the total tunneling rate (Γ_l and Γ_r are the tunneling rates to the source and the drain), which enter in equation (1).

Figure 1 shows the temperature dependence of few Coulomb blockade resonances. The left panel is for a resonance at low gate voltage. The temperature dependence of the resonant line is in accordance with the thermally broadened resonant tunneling regime where the intrinsic elastic broadening of the line $h\Gamma$ is much less than the temperature and/or the inelastic broadening $h\Gamma_{in}$. At temperature above 300 mK, the full width at half maximum (FWHM) ΔV_G varies linearly with the temperature in accordance with the prediction: $\alpha e \Delta V_G \simeq 3.5 k_B T$ and $\alpha = 0.28$ is the conversion factor between gate voltage and Fermi energy variations [13]. Below 200 mK the FWHM saturates to a value corresponding to an effective temperature of 170 mK, which could be either an effective electronic temperature or $\frac{h\Gamma_{in}}{k_B}$. In any case the temperature is much smaller than $\Delta \simeq 1$ meV and $U \simeq 2$ meV. The resonant conductance in units of e^2/h is approximately equal to $G_{res} = 0.02$. $G_{res} = \frac{h\Gamma}{\max(k_B T, h\Gamma_{in})}$ if $\Gamma_l \simeq \Gamma_r \simeq \Gamma/2$ or $G_{res} = \frac{h\Gamma_{l(r)}}{\max(k_B T, h\Gamma_{in})}$ if $\Gamma_{l(r)} \ll \Gamma_{r(l)}$, such that $G_{res} \ll 1$ means that one of the tunneling rates at least is small. In this regime, where cotunneling is weak, we observe Coulomb blockade with usual behaviour for temperature or drain-source voltage dependence (see Fig. 2): in the off-resonance regime, the lowest is the temperature or the transport drain-source voltage, the smallest is the drain-source current (or conductance), as expected due to the presence of the Coulomb blockade activation gap (and negligible cotunneling effect).

Figure 2 shows the stability diagram in this low gate voltage regime. Light gray rhombuses, *i.e.* regions where drain-source current is negligible, correspond to an energy ground state with a fixed number of electrons in the dot. These regions have not the same surface, because Δ is not negligible as compared to U (contrarily to the orthodox model of Coulomb blockade) and the rhombuses diameter is $U + \Delta$ (instead of U). At zero drain-source

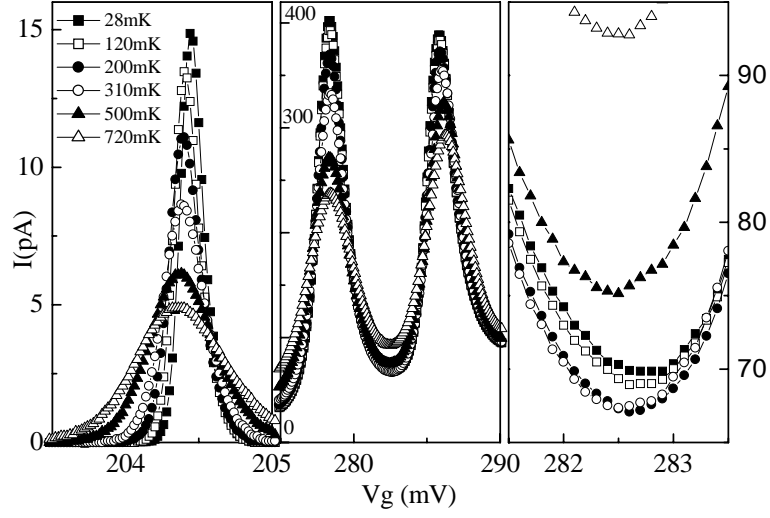


Fig. 1. Temperature dependence of the Coulomb blockade peaks. The drain-source voltage is $20 \mu\text{V}$. Left panel: weakly coupled regime; Center panel: strongly coupled regime; Right panel: detail of the region between the two peaks in the strongly coupled regime (noted K_3 in Fig. 5) with the anomalous temperature dependence below $T = 300 \text{ mK}$.

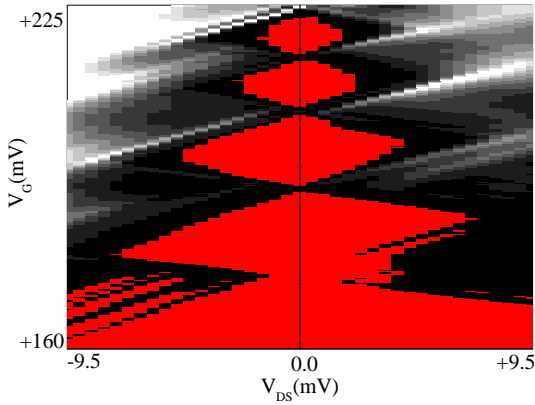


Fig. 2. Contour plot of the drain-source differential current I_{DS} versus drain-source voltage (horizontal axis) and gate voltage (vertical axis). The a.c. drain-source voltage is $20 \mu\text{V}$. Each gray correspond to a $I_{DS} = 5 \text{ pA}$ step (from 0 pA – 5 pA (light gray), 5 Pa – 10 Pa (black),..., to $\geq 50 \text{ pA}$ (white). The range of gate voltage corresponds to a weak coupling between the electrons at the bottom of the impurity quantum dot (IQD) and the electrodes. The size of the diamond shape Coulomb blockade rhombus is larger at smaller gate voltage, reflecting the large mean level spacing Δ at the bottom of the IQD. $\Delta \simeq 1 \text{ meV}$ appears also as the eV_{DS} spacing between the lines, corresponding to drain-source conductance by excited states outside the Coulomb blocked rhombuses. The four rhombuses are labelled as four N (normal regions) in Figure 5.

voltage, the rhombuses merge at degeneracy points where ground states with N and $N + 1$ electrons in the dot are degenerate, and a drain-source current passes through the IQD. Because the experiment is performed at temperature and $h\Gamma$ less than the mean level spacing Δ , outside the Coulomb blocked rhombuses, we observe the excited states of the IQD at finite drain-source voltage. This appears as maximum differential conductance lines parallel to the borders of the rhombuses for the first resonances,

and permits to evaluate the mean level spacing $\Delta \simeq 1 \text{ meV}$ at the bottom of the confinement potential [13].

When the gate voltage is increased further, electrons are injected in the channel at higher energy and populate the top of the IQD potential. The Coulomb blockade peaks show a more regular separation in energy (or gate voltage), reflecting a smaller Δ/U ratio (see Fig. 5). Δ decreases at large electronic energies because either the IQD confinement potential is less steep than parabolic at high energies, and/or the density of states is not constant, but increases with energy in the Lifshitz tail of the conduction band (*i.e.* the density of states at the bottom of the conduction band is not constant but increases exponentially with energy due to disorder) [16]. A consequence of this smaller Δ is that the excited states are no more resolved at finite drain-source voltage, as expected if $h\Gamma \simeq \Delta$. Δ is still larger than $k_B T$ as proved by the temperature dependence of the Coulomb blockade peaks: the drain-source current at the resonance increases as the temperature decreases (below $T = 4.2 \text{ K}$), that characterizes the thermally broadened resonant tunneling regime, $\Delta \geq k_B T$ (by contrast to the orthodox model of Coulomb blockade, where $\Delta \ll k_B T$) (see Fig. 1, center panel).

Γ increases also with gate voltage, because the effective height for the electrostatic barriers forming the tunnel contacts to the electrodes decreases with the gate voltage (in IQDs there is no separate gate to control the tunneling rates Γ_l and Γ_r). For large enough gate voltage the channel of the MOSFET is open, and the drain-source conductance is larger than e^2/h . For gate voltage $250 \text{ meV} \leq V_G \leq 350 \text{ mV}$ typically, below the opening of the channel, we estimate that $h\Gamma \simeq \Delta \simeq 0.6 \text{ meV}$. The resonant conductance is close to e^2/h . $h\Gamma$ could be obtained from the FWHM of the Coulomb blockade peaks in figures 1 (right panel) and 5: the FWHM is typically $\Delta V_G = 2.5 \text{ mV}$ ($\alpha \simeq 0.28$) at the lowest temperature and is almost independent of the temperature below $T = 310 \text{ mK}$. The charging energy is $U \simeq 2 \text{ meV}$

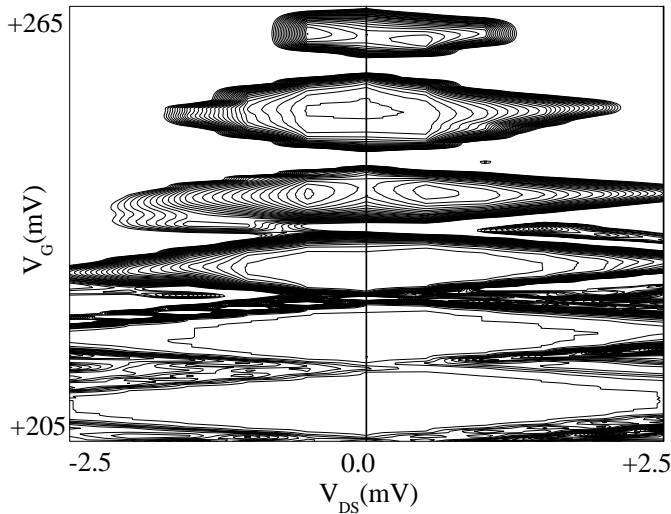


Fig. 3. Enlarged Contour plot of the drain-source differential conductance *versus* drain-source voltage (horizontal axis) and gate voltage (vertical axis). The a.c. drain-source voltage is 20 μV . Each contour line is separated by 1 pA (from 1 pA to 30 pA). Currents below 1pA in the first three rhombus (at low V_G) appear in white, as well as currents above 30 pA for the degeneracy points or at large drain-source voltage outside the rhombuses. Note the sequence of two maxima/minima of differential conductance appearing near zero bias inside the four top rhombuses (at large V_G). The two maxima are labelled K_1 and K_2 in Figure 5.

($U = \alpha e/C_G \simeq \alpha \times 8 \text{ mV}$) We can conclude that $\frac{U}{h\Gamma}$ is of order of a factor 3.5 in our samples. This factor is just the ratio between the FWHM and the peak spacing in gate voltage in Figure 1 (center panel). Such $\frac{U}{h\Gamma}$ is comparable to what has been reported typically in GaAs structures or in carbon nanotubes where Kondo effect has been observed (see later on). With this estimation, the exponential factor in equation 1 is about $\exp(-\frac{\pi}{4}(\frac{2 \text{ meV}}{0.6 \text{ meV}})) \simeq 7 \times 10^{-2}$, giving a Kondo temperature of order $k_B T_K \simeq 35 \mu\text{eV}$ (or $T_K \simeq 400 \text{ mK}$).

We indeed observe features, the Kondo ridges, which are signature of the Kondo effect for valleys of conductance (noted K_1 to K_4 in Fig. 5), at temperature below $T = 400 \text{ mK}$ and drain source-voltages below $\simeq 100 \mu\text{eV}$ (see Figs. 3 and 4). The Kondo ridges are lines of local maximum conductance near $V_{DS} \simeq 0$, appearing in the stability diagram regions corresponding to an odd number of electrons in the IQD (noted by “K” for Kondo). They contrast with the local minimum of conductance near $V_{DS} \simeq 0$ observed in regions with an even number of electrons in the IQD (noted by “N” for normal). The effect we observe is small in amplitude, of order few percents. For the temperature dependence shown on the right panel of Figure 1 and on the inset Figure 5 for K_3 and K_4 , the upturn of the drain-source current below $T = 310 \text{ mK}$ is of order 4 percents, two orders of magnitude larger than our experimental sensitivity. For the drain-source voltage dependence of K_4 plotted in Figure 4, the upturn is 5 percents ($I_{DS} = 38.1 \text{ pA}$ on the Kondo ridge at $V_{DS} \simeq 0 \mu\text{V}$ against 36.1 pA at $V_{DS} = 150 \mu\text{V}$).

The typical drain-source voltage V_{DS}^* to suppress the Kondo effect is obtained from Figures 3 and 4: $eV_{DS}^* \simeq 100 \mu\text{eV} \geq k_B T_K \simeq 20 \mu\text{eV}$. In previous reports, $eV_{DS}^* \geq k_B T_K$ have been also reported (see later on and [7]). Due to the restricted range of variation for $G(T)$ and $G(V)$, it is not possible to extract a reliable estimation of T_K . The small temperature variation is compatible with a logarithmic behavior in temperature, expected near the Kondo temperature [17] (not shown). We observe a saturation of the temperature dependence below $T \simeq 0.15 \text{ K}$, that could be due to an overheating of electrons by radiofrequency pickup, because the temperature dependence is also weak below $T = 150 \text{ mK}$ at low gate voltage (see previous discussion for the weakly coupled regime and left panel of Fig. 1). This saturation could limit somewhat the amplitude of the Kondo resonance.

The Kondo temperature is small in our devices, less or at least comparable to 1 kelvin, but close to our estimation based on equation 1. This rough accordance is satisfactory and compares well with previous reports on Kondo effect, which show some dispersivity for U , Δ , Γ and T_K :

Goldhaber-Gordon *et al.* report [17]: $U \simeq 1.96 \text{ meV}$, $h\Gamma \simeq 0.3 \text{ meV}$, $\Delta \simeq 0.4 \text{ meV}$ and $T_K \simeq 40 \text{ mK}$ (in the middle of the odd valleys) for 150 nm GaAs dot. Cronenwett *et al.* obtain [2]: $U \simeq 0.5 \text{ meV}$, $h\Gamma \simeq \Delta \simeq 0.10 - 0.15 \text{ meV}$ and $T_K \simeq 1000 \text{ mK}$ in 300 nm GaAs dot (170 nm diameter after taking into account depletion effects). T_K is determined from the bias voltage dependence of the Kondo resonance: $eV_{DS} \simeq k_B T_K \simeq 100 \mu\text{eV}$, but the upturn of the conductance at low temperature occurs for $T \leq 200 \text{ mK}$. Simmel *et al.* [5] have $U \simeq 2.7 \text{ meV}$, $\Delta \simeq 0.5 \text{ meV}$, $h\Gamma \simeq 0.1 \text{ meV}$ and $T_K \simeq 20 \text{ mK}$ (in the middle of the odd valleys) for 140 nm diameter GaAs dot. In vertical, strongly coupled GaAs artificial dots [4], $T_K \simeq 350 \text{ mK}$. Finally, in carbon nanotubes [7], $U/\Delta \simeq 6$ and $\Delta \simeq 0.2 \text{ meV}$ and $T_K \simeq 0.9 - 1.6 \text{ K}$. Despite the dispersivity on U , $h\Gamma$, Δ , U/Γ is always comparable to 5.

Although our system is rather different than artificial GaAs structures or carbon nanotubes, the pertinent parameters U , $h\Gamma$, Δ and T_K are of the same order of magnitude, stressing the generality of the physics but also the limited range of parameters accessible in experiments.

As mentioned before the Kondo resonance is related to the total spin in the dot. Anomalies in the even-odd sequence are nevertheless expected in models which deviate from the constant charging energy case and include the exchange energy [6]. In our IQD, we follow the alternance of 3 couples of odd-even valleys, followed by an anomaly labelled by two question marks in Figures 4 and 5: for these two valleys the temperature dependence is very flat below $T = 400 \text{ mK}$. It is not possible to label these valleys by normal or Kondo. Flat behaviors have also been reported GaAs artificial dots [2]. Correlatively to the temperature dependence, the voltage dependence is intermediate between what is observed in normal and Kondo valleys for $V_{DS} \leq 150 \mu\text{V}$. Analysis of the non linearities shows a non symmetric behavior of the drain-source current with drain-source voltage polarity (see Fig. 4). This is due to non equal Γ_l and Γ_r tunneling rates. Non

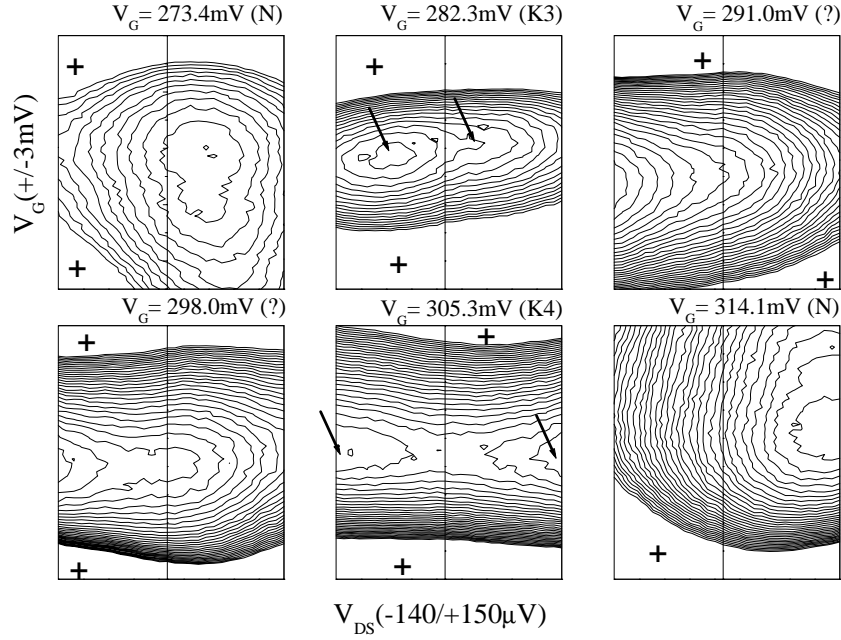


Fig. 4. Detailed contour plots of the drain-source current *versus* drain-source voltage (horizontal axis) and gate voltage (vertical axis) for the valleys of conductance. The a.c. drain-source voltage is $10 \mu\text{V}$. The vertical line indicates zero DC drain-source voltage. Each contour line is separated by 1 pA . Top left panel: V_G varies from 270.4 mV ($273.4 \text{ mV} - 3 \text{ mV}$) to 276.4 mV ($273.4 \text{ mV} + 3 \text{ mV}$); contour lines go from 14 pA to 25 pA separated by 1 pA . Regions where current is above 25 pA are indicated by a $+$ symbol. Top middle panel: V_G varies from 279.3 mV to 285.3 mV ; contour lines go from 34 pA to 50 pA . Top right panel: V_G varies from 288.0 mV to 294.0 mV ; contour lines go from 42 pA to 70 pA . Bottom left panel: V_G varies from 295.0 mV to 301.0 mV ; contour lines go from 43 pA to 70 pA . Bottom center panel: V_G varies from 302.3 mV to 308.3 mV ; contour lines go from 37 pA to 65 pA . Bottom right panel: V_G varies from 311.1 mV to 317.1 mV ; contour lines go from 15 pA to 55 pA . A Kondo ridge appear near zero drain-source voltage, in the valley labelled K_3 and K_4 . For these valleys two minima of conductance indicated by arrows are located across the $V_{DS} = 0$ line. For these two valleys, the linear conductance increases below $T \simeq 400 \text{ mK}$ (see inset of Fig. 5). For the two valleys noted normal (N), the linear conductance decreases with temperature decreasing as usual in Coulomb blockade regime. A single minima in non linear current appears which is eventually shifted from the $V_{DS} = 0$ line. The two valleys indicated by a question mark show a flat temperature dependence of the linear conductance at low temperature. Contour plots are somewhat intermediate between normal and Kondo valleys, with a single local minimum for the non linear current (as in N), but a flatness of the contour lines for the opposite V_{DS} polarity.

equal tunneling rates are the rule in our IQD (where there is no separate gate control and where the transparencies change with gate voltage), and explain several non-symmetrical features both in the strongly and weakly connected regimes [18]. Kondo anomalies at finite bias have been reported in non-symmetrical artificial dots [5], and observed in IQD [11]. This demonstrates that Kondo resonance is affected by the ratio between the two tunneling rates, and possibly offset from $V_{DS} = 0$. In our sample, a clear Kondo behavior is defined near $V_{DS} = 0$, if two local minima for the current exist, one for each polarities (valleys K_3 and K_4 ; see also K_1 and K_2 on figure 3). On the contrary a normal behavior is associated with a single minima, eventually shifted from $V_{DS} = 0$. An ambiguous behavior appears when a single minima exists for one polarity and a second minima is not resolved, but only revealed by a flatness of the non linearity near $V_{DS} = 0$.

Note that the valley K_4 is Kondo like in disagreement with the strict parity for electron number in the dot, the next one is normal. But alternate sequences longer than 3 Kondo-normal pairs in gate voltage have not been

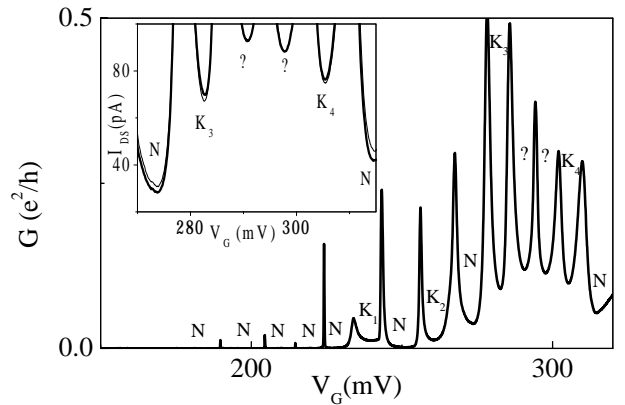


Fig. 5. Coulomb blockade pattern: N means normal dependence (both in temperature and drain-source voltage), K means Kondo dependence and a question mark indicates that both temperature and bias dependence are very flat in the low energy range. Inset: Source-drain current (excitation $20 \mu\text{V}$) *versus* gate voltage for two temperatures (310 mK , thin line, and 35 mK , thick line). Note the increase of conductance at very low temperature in regions labelled K_3 and K_4 .

reported previously to our knowledge neither in GaAs structures or in carbon nanotubes. Observation of longer alternate sequences is still a challenge. This indicates the limits of a simple Pauli picture for filling a quantum dot with electrons and the importance of exchange interaction. We note also that the twofold valley degeneracy in inversion layer of silicon MOSFETs could induce a spin polarization of the ground state with total spin larger than $1/2$ (Hund's rule), and consequently a suppression of the Kondo-normal alternance.

In summary we observed signatures of the Kondo effect in silicon impurity quantum dot. The Kondo temperature is less than one kelvin, as expected from estimations for charging energy, mean level spacing and tunneling rate. The Kondo resonance manifestations are similar to other previous reports. It indicates that the Kondo effect is not restricted to artificial quantum dot or carbon nanotubes, but also exists in functional silicon MOSFETs, the prototypes of microelectronics.

We greatly acknowledge the use of the LETI-PLATO facility for fabricating the Silicon MOSFETs.

References

1. D. Goldhaber-Gordon *et al.*, Nature **391**, 156 (1998).
2. S.M. Cronenwett, T.H. Oosterkamp, L.P. Kouwenhoven, Science **281**, 540 (1998).
3. J. Schmid, J. Weis, K. Eberl, K. Von Klitzing, Physica B **256-258**, 182 (1998).
4. S. Sasaki *et al.*, Nature **405**, 764 (2000).
5. F. Simmel *et al.*, Phys. Rev. Lett. **83**, 804 (1999).
6. J. Schmid, J. Weis, K. Eberl, K. Von Klitzing, Phys. Rev. Lett. **84**, 5824 (2000).
7. J. Nygard, D.H. Cobden, P.E. Lindelof, Nature **408**, 342 (2000).
8. L. Kouwenhoven, L. Glazman, Phys. World **14**, 33 (2001).
9. W.G. Van der Wiel *et al.*, Science **289**, 5225 (2000).
10. D.V. Averin, Yu. V. Nazarov, in *Single Charge Tunneling*, edited by H. Grabert, M.H. Devoret (Plenum Press, New York 1992).
11. L.P. Rokhinson, L.J. Guo, S.Y. Chou, D.C. Tsui, Phys. Rev. B **60**, R16319 (1999).
12. L.P. Rokhinson, L.J. Guo, S.Y. Chou, D.C. Tsui, Phys. Rev. B **63**, 035321 (2001).
13. M. Sanquer *et al.*, Phys. Rev. B **61**, 7249 (2000).
14. A.I. Larkin, K.A. Matveev Sov. Phys. JETP **66**, 580 (1987).
15. H. van Houten, C.W.J. Beenakker, A.A.M. Staring, in *Single Charge Tunneling*, edited by H. Grabert, M.H. Devoret (Plenum Press, New York 1992).
16. The experimental $\alpha = \frac{\Delta\mu_F}{e\Delta V_g}$ parameter is a factor of 5 larger than calculated with the 2DEG density-of-states $\rho_{2DEG} = m^*/\pi\hbar^2$ and the gate capacitance $C_G \simeq 10^{-14} \text{ F}\mu\text{m}^{-2}$, reflecting that the density-of-states at low energy (in the Lifshitz tail) is effectively reduced.
17. D. Goldhaber-Gordon *et al.* Phys. Rev. Lett. **81**, 5225 (1998).
18. The tunnel transparencies are also strongly affected by a magnetic field, such that the fine analysis of the Kondo ridge with magnetic field applied is very difficult and has not been performed here.